ACS OMEGA

Open Access



http://pubs.acs.org/journal/acsodf

Article

# High-Pressure Synthesis and Structural Studies of La, Sm, Gd, and Dy Chlorides and Chloride Carbides

Fariia Iasmin Akbar,* Alena Aslandukova, Andrey Aslandukov, Yuqing Yin, Elena Bykova, Maxim Bykov, Dominique Laniel, Pavel Milkin, Timofey Fedotenko, Jonathan Wright, Anna Pakhomova, Gaston Garbarino, Mohamed Mezouar, Michael Hanfland, Natalia Dubrovinskaia, and Leonid Dubrovinsky*

Cite This: *ACS Omega* 2026, 11, 4280−4289

Read Online

ACCESS | Metrics & More | Article Recommendations | Supporting Information

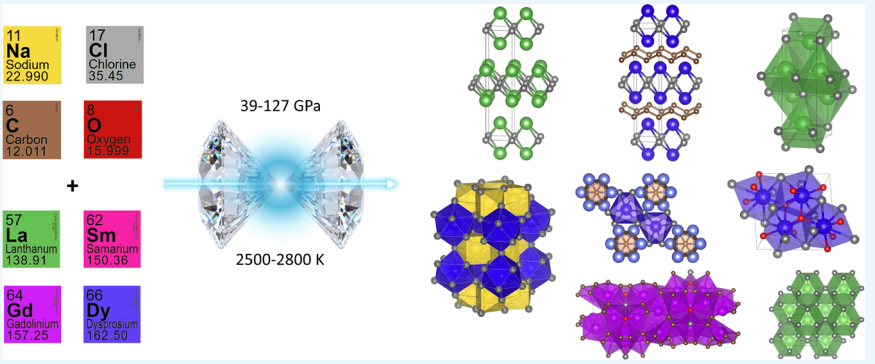


**ABSTRACT:** High-pressure synthesis provides unique pathways to materials with unprecedented structures and properties. Here we report the synthesis and structural characterization of novel rare-earth (La, Sm, Gd, Dy) chlorides, chloride carbides, and oxychloride phases obtained due to complex chemical reactions in diamond anvil cells after laser heating of rare-earth metals and NaCl at pressures of 39−127 GPa and temperatures of 2500−2800 K. Synchrotron single-crystal X-ray diffraction analysis allowed us to solve previously unknown crystal structures of binary ($La_2Cl$, LaCl, $LaCl_3$, DyCl) and ternary ($DyNa_2Cl_5$, $Sm_2ClC_2$, $Gd_2ClC_2$, $Dy_2ClC_2$, $Sm_{19}ClC_{18}$, $Gd_{19}ClC_{18}$, $Dy_5Cl_3C$, DyOCl) compounds. Significantly, we identified *trans*-polyacetylene-like carbon chains in lanthanide chloride carbides, a structural motif previously hypothesized but not observed experimentally. Our findings highlight the enhanced chemical reactivity of alkali halides under extreme conditions, uncovering novel chemical bonding and expanding the landscape of potential functional materials accessible through high-pressure synthesis.

## INTRODUCTION

Rare-earth element (REE) chlorides and chloride carbides are of considerable interest in science and technology due to their distinctive physical and chemical properties, which enable a wide range of applications. REE chlorides serve as essential precursors in materials synthesis,[1] metallurgy,[2] and catalysis,[3] while chloride carbides—though less explored—exhibit intriguing structural diversity and potential for advanced functional materials.[4,5] Their unique electronic,[6] magnetic,[7] and optical properties make them valuable in fields such as optics,[8] energy storage,[9,10] and catalysis.[11,12] Understanding and harnessing these compounds can lead to advancements in cutting-edge technologies, including superconductors, fuel cells, and environmental remediation strategies.

REE chlorides and chloride carbides can be synthesized by several established methods. Direct chlorination and carbochlorination of $REE_2O_3$ with chlorine gas at high temperatures (in the presence of carbon in the case of carbochlorination) yield anhydrous $REECl_3$.[13] Chloride carbides (REE−Cl−C) are typically obtained via solid-state reactions involving REEs, graphite, and REE trichlorides ($REECl_3$) under an inert atmosphere at high temperatures.[14−16] Another example is hydrothermal synthesis, which is particularly useful for creating layered and high-entropy REE compounds with controlled stoichiometry and crystal structures.[17] While these methods are well-known, high-pressure synthesis in laser-heated diamond anvil cells (DACs) using Cl-bearing precursors remains an emerging approach, offering the potential for novel REE phases with unique properties.

Received: September 9, 2025
Revised: December 11, 2025
Accepted: January 6, 2026
Published: January 9, 2026

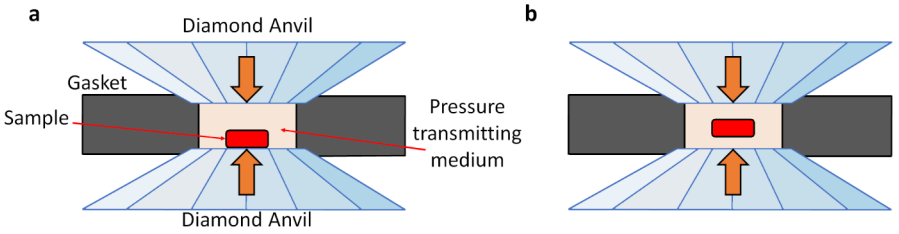


**Figure 1.** A schematic representation of the cross-section of the pressure chamber showing different sample loading geometries. (a) Thin pieces of a metal are placed directly on a diamond anvil (used in the current study). (b) The metal is isolated from the anvils by the pressure medium.

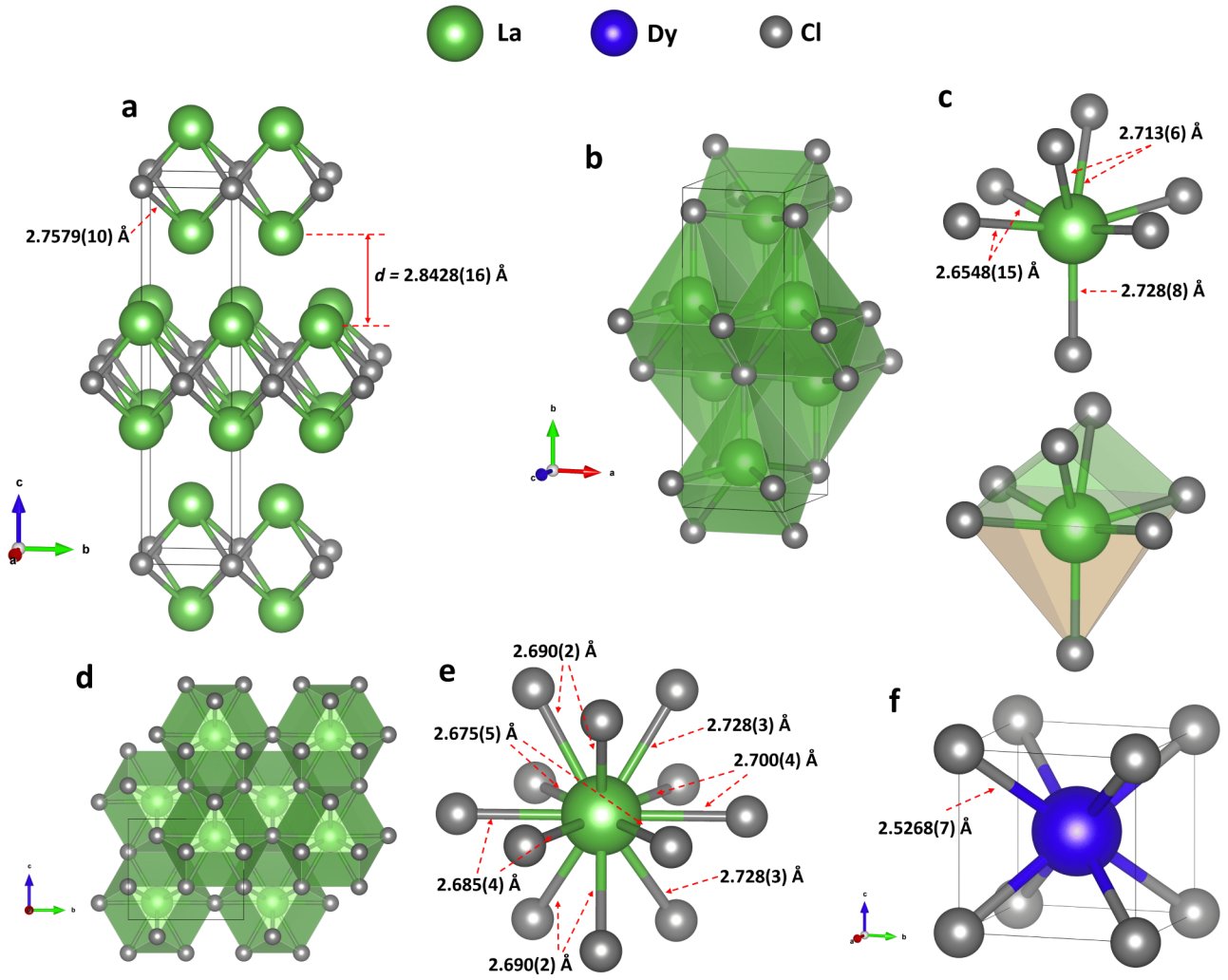


**Figure 2.** Crystal structures of the newly synthesized lanthanum and dysprosium chlorides. (a) *tI*6 $La_2Cl$ at 81(2) GPa, stick-and-ball model. (b) *oC*8 LaCl at 80(2) GPa, polyhedral model; (c) coordination of La atoms with interatomic distances (top) and highlighted polyhedron shape (bottom). (d) *oP*8 $LaCl_3$ at 81(2) GPa, polyhedral model viewed along the *a* direction; (e) coordination of La atoms. (f) *cP*2 DyCl at 95(3) GPa, a unit cell. Green, gray, and blue spheres represent lanthanum, chlorine, and dysprosium atoms, respectively; unit cells are outlined by thin black lines.

In the present work, we report the synthesis and structural studies of chlorides, chloride carbides, and oxychlorides of La, Sm, Gd, and Dy, obtained due to chemical reactions of REEs with NaCl during laser heating in DACs at pressures of 39 to 127 GPa. All compounds were analyzed *in situ* at high pressures by using synchrotron single-crystal X-ray diffraction (SCXRD). Crystal structures of many previously unknown binary (*tI*6 $La_2Cl$, *oC*8 LaCl, *oP*8 $LaCl_3$, and *cP*2 DyCl) and ternary compounds (*oI*32 $DyNa_2Cl_5$, *oC*10 $Sm_2ClC_2$, *oC*10 $Gd_2ClC_2$, *oC*10 $Dy_2ClC_2$, *mP*76 $Sm_{19}ClC_{18}$, *mP*76 $Gd_{19}ClC_{18}$, *hP*18 $Dy_5Cl_3C$, and *oP*12 DyOCl) have been solved and refined. Our work contributes to the development of synthesis methods for lanthanide chlorides and chloride carbides, extending knowledge of their crystal structures and crystal chemistry.

## MATERIALS AND METHODS

### Sample Preparation

In our experiments, we utilized BX90-type DACs with a large X-ray aperture.[18] We employed Boehler-Almax-type diamonds as anvils with



https://doi.org/10.1021/acsomega.5c09373
ACS Omega 2026, 11, 4280−4289

culet diameters of 80/120/250 μm. Rhenium gaskets with an initial thickness of 200 μm were indented to ~16/22/28 μm, and a hole of ~35/55/105 μm in diameter was laser-drilled in the center of the indentation. Thin pieces of metals (Sc, Y, La, Sm, Gd, or Dy; 99.9%, ChemPur or smart-elements) were placed directly on the diamond anvil (Figure 1a) and covered by dry sodium chloride, NaCl (99.999% purity, ChemPUR) which served as a thermal insulator, pressure-transmitting medium, and reactant. Contact with the diamond anvil enabled a carbon source for chemical reactions with the metals. There is another way to place the metal in the DAC so that it is isolated from the anvils by the pressure-transmitting medium (Figure 1b). Although we did not use this configuration, we discuss below how the different arrangements affect the experimental results.

Samples were compressed to the desired pressure and laser-heated at 2500(200)−2800(200) K using an *in-house* double-sided YAG laser-heating setup[19] (1064 nm wavelength). Thermal emission spectra from the heated area were collected using an IsoPlane SCT 320 spectrometer with a 1024 × 2560 PI-MAX 4 camera.[19] The pressure was determined using the NaCl equation of state (EoS).[20,21]

### X-ray Diffraction

The reaction products were analyzed by synchrotron single-crystal X-ray diffraction (SCXRD) measurements at the P02.2 beamline ($\lambda$ = 0.2904 Å, beam size ~ 1.5 × 2 $\mu m^2$) of Deutsches Elektronen-Synchrotron (DESY, PETRA III, Hamburg, Germany) and at three synchrotron beamlines of the European Synchrotron Radiation Facility (ESRF, Grenoble, France): ID11 ($\lambda$ = 0.2846 Å, beam size ~ 0.75 × 0.75 $\mu m^2$), ID15B ($\lambda$ = 0.4100 Å, beam size ~ 1.5 × 2 $\mu m^2$), and ID27 ($\lambda$ = 0.3738 Å, beam size ~ 2 × 2 $\mu m^2$). At the P02.2 beamline of DESY, diffraction patterns were collected on a PerkinElmer 1621 XRD flat-panel detector. At the ID11 beamline of the ESRF, data acquisition was performed with an Eiger2X CdTe 4 M hybrid photon-counting pixel detector, while at ID15B and ID27, an Eiger2X CdTe 9 M hybrid photon-counting pixel detector was used. Powder X-ray diffraction (PXRD) images were collected upon continuous sample rotation in a range of ±1° around the vertical $\omega$ axis. During single-crystal data collection, the cell was rotated around the vertical $\omega$ axis from −38° to +38° with narrow 0.5° steps. Creating maps with XDI software[22] helps to visualize the phase distribution within the pressure chamber and to locate areas where the SCXRD data collections should be performed. The CrysAlis$^{Pro}$ software package[23] was used for the analysis of the SCXRD data (peak hunting, indexing, data integration, frame scaling, and absorption correction). To calibrate an instrument model in the CrysAlis$^{Pro}$ software, i.e., the sample-to-detector distance, the detector's origin, offsets of the goniometer angles, and rotation of both the X-ray beam and the detector around the instrument axis, we used a single crystal of orthoenstatite [$(Mg_{1.93},Fe_{0.06})(Si_{1.93},Al_{0.06})O_6$, *Pbca* space group, $a$ = 8.8117(2) Å, $b$ = 5.18320(10) Å, and $c$ = 18.2391(3) Å]. The DAFi program was used for the search of reflection groups belonging to the individual single-crystal domains.[24] Using the OLEX2 software package,[25] the structures were solved with the ShelXT structure solution program[26] using intrinsic phasing and refined with the ShelXL[27] refinement package using least-squares minimization. Crystal structure visualization was made with VESTA software.[28] The polyhedral assignments were made according to the fitting results obtained using Polynator software.[29]

## RESULTS AND DISCUSSION

The experimental details are summarized in Table S1 (Supporting Information). In addition to chlorides, chloride carbides, and oxychloride (the latter formed due to partial oxidation of Dy during sample loading), we observed the formation of numerous carbides. The results of the carbide studies will be published separately.

In this paper, we describe all newly identified chlorine-containing phases, beginning with binary and ternary chlorides, followed by chloride carbides—ordered by increasing chlorine content per formula unit—and concluding with an oxychloride. A general discussion follows the phase descriptions.

### Structures of Novel Lanthanide Chlorides

**Lanthanum Chlorides.** In the DAC loaded with La and NaCl, three lanthanum chloride phases were detected as products of chemical reactions (Tables S1 and S2).

The previously unknown *tI*6 $La_2Cl$ phase, discovered at 81(2) GPa, has a tetragonal unit cell (space group *I*4/*mmm*, #139, $Z$ = 2, Table S2), in which four lanthanum atoms occupy the 4*e* Wyckoff site and two chlorine atoms occupy the 2*a* positions (Figure 2a, Table S2). In the structure of *tI*6 $La_2Cl$ (Figure 2a) (anti-$LaI_2$ structure,[30] $MoSi_2$ structure type[31] ($CuZr_2$-type according to the ICSD database[32])), each La atom is connected to four Cl atoms at a distance of 2.7579(12) Å. In a simple geometrical representation of the structure, the $La_2Cl_4$ groups form octahedra, and these octahedra are connected through Cl−Cl edges to form layers. The layers are packed in an ABAB··· sequence and are shifted by 1/2 of the diagonal of the octahedra relative to each other. To the best of our knowledge, $Y_2Cl$ is the only other rare-earth chloride with a $REE_2Cl$ stoichiometry reported to date, having been both theoretically predicted[33] and experimentally synthesized.[4] Despite their identical stoichiometries, $Y_2Cl$ and $La_2Cl$ adopt different crystal structures.

The lanthanum monochloride *oC*8 LaCl (space group *Cmcm*, #63, $Z$ = 4, Table S2) synthesized at 80(2) GPa has the TlI structure type (B33).[34] The previously known *hR*12 LaCl polymorph[35] has the ZrCl-type structure (space group *R*-3*m*, #166, $Z$ = 6). The *oC*8 LaCl orthorhombic unit cell contains lanthanum and chlorine atoms occupying Wyckoff site 4*c* (Figure 2b). Lanthanum atoms are coordinated by seven chlorine atoms at distances of either 2.6548(15), 2.713(6), or 2.728(8) Å in the capped trigonal prismatic molecular geometry, forming a kind of an augmented triangular prism (or monocapped isosceles wedge, according to the Polynator fitting[29])—a polyhedron constructed by attaching a pyramid onto the rectangular face of a triangular prism (shown in orange and green, respectively) (Figure 2c). The apexes of the prisms are alternately oriented in two opposite directions along the *b*-axis as shown in Figure 2b; the trigonal prisms share faces, whereas the pyramids share edges.

The lanthanum trichloride *oP*8 $LaCl_3$ crystallized at 81(2) GPa. Its orthorhombic structure (space group *Pmmn*, #59, $Z$ = 2) has not been observed previously. The other known polymorph, *hP*2 $LaCl_3$,[36] has the $UCl_3$-type structure (space group $P6_3/m$, #176, $Z$ = 2). In the structure of *oP*8 $LaCl_3$ (isostructural to $LaF_3$, anti-$Cu_3Ti$ structure type[37] ($\beta$−$TiCu_3$-type according to the ICSD database[32])), lanthanum atoms occupy a single 2*a* Wyckoff position. They are coordinated by twelve chlorine atoms (on the 4*e* (Cl1) and 2*b* (Cl2) Wyckoff sites) at distances of 2.675(5)-2.728(3) Å (Figure 2d, e, Table S2), forming an anticuboctahedron polyhedron—composed of eight triangular and six square faces. The polyhedra form columns along the *b* direction through corner sharing. The columns are interconnected through sharing of triangular and square faces.

### Dysprosium Chlorides

The dysprosium monochloride, *cP*2 DyCl, was synthesized at pressures of 95(3) and 121(3) GPa, differing from the previously discovered *hP*4 DyCl at 40 GPa[4] (NiAs-type structure, space group $P6_3/mmc$, #194, $Z$ = 2). This novel compound has a CsCl-type structure (space group *Pm*-3*m*,


https://doi.org/10.1021/acsomega.5c09373
ACS Omega 2026, 11, 4280−4289

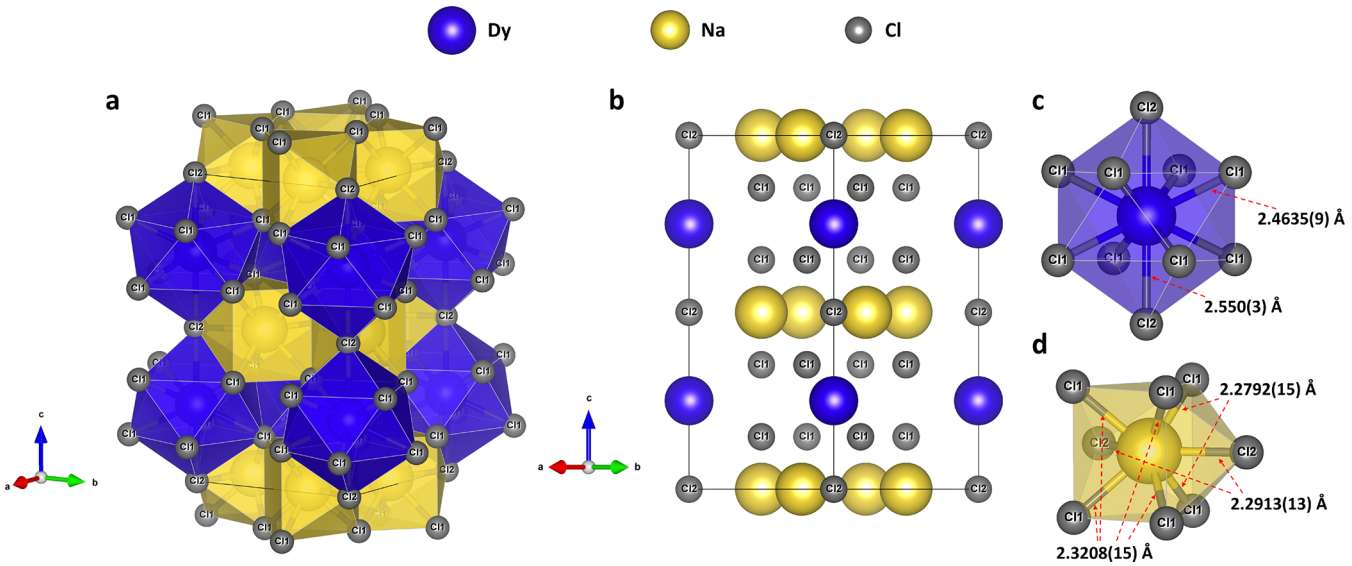


**Figure 3.** Crystal structure of *oI*32 $DyNa_2Cl_5$ at 107(3) GPa. (a) A polyhedral model. (b) A ball model viewed along the [110] direction. Coordination of the (c) Dy and (d) Na atoms. Dysprosium—blue, sodium—yellow, and chlorine—gray.

#221, $Z = 1$), with chlorine and metal atoms occupying 1*a* and 1*b* Wyckoff positions, respectively (Table S3). Dysprosium atoms are coordinated by the eight nearest chlorine atoms with a Dy−Cl distance of 2.5268(7) Å at 95(3) GPa (Figure 2f).

The novel dysprosium−sodium chloride *oI*32 $DyNa_2Cl_5$ (*I*4/*mcm*, #140, $Z = 4$) with the $NH_4Pb_2Br_5$-type structure[38−40] ($RbPb_2Br_5$-type according to the ICSD database[32]) was observed at 107(3) GPa (Figure 3, Table S4) among the products of high-pressure high-temperature (HPHT) reaction between Dy and NaCl. The Dy, Cl1, Cl2, and Na atoms occupy the 4*a*, 16*l*, 4*c*, and 8*h* Wyckoff sites, respectively. Dysprosium atoms are coordinated by ten chlorine atoms at distances of *d*(Dy1−Cl1) = 2.4635(9) Å and *d*(Dy1−Cl2) = 2.550(3) Å at the synthesis pressure (Figure 3c), forming a bicapped tetragonal antiprism. Sodium atoms are in a bicapped trigonal prism formed by eight chlorine atoms with interatomic distances of *d*(Na1−Cl1) = 2.2792(15) or 2.3208(15) Å and *d*(Na1−Cl2) = 2.2913(13) Å (Figure 3d). The phases with the $NH_4Pb_2Br_5$-type structure are described in the literature[38−40] by the general formula $Me1^{+}(Me2^{2+})_2X^{-}$, where Me1 and Me2 are electropositive, and X is an electronegative atom. In *oI*32 $DyNa_2Cl_5$, Me1 = $Dy^{3+}$ and Me2 = $Na^{+}$ which makes it distinct from previously known compounds.

## Structures of Rare-Earth Metal Chloride Carbides

**Chloride Carbides with the $Mn_2AlB_2$-Type Structure.** Three rare-earth ternary compounds, *oC*10 $REE_2ClC_2$ (REE = Sm, Dy, Gd), synthesized in this work, exhibit the $Mn_2AlB_2$-type structure (space group *Cmmm*, #65, $Z = 2$) previously known mainly for borides,[41,42] but unknown for carbides and chlorides. Their orthorhombic unit cells contain REE, chlorine, and carbon atoms located at the 4*j*, 2*a*, and 4*i* Wyckoff sites, respectively (Figure 4a, Table S5). Carbon atoms form *trans*-polyacetylene-like chains along the *a*-axis with a C−C distance of 1.549(14) Å and an angle ∠(C−C−C) = 123.9(19)°.

**Chloride Carbides with $Sm_{19}ClC_{18}$-Type Structure.** The rare-earth chloride carbides *mP*76 $Sm_{19}Cl_{0.81}C_{18}$ and *mP*76 $Gd_{19}ClC_{18}$ ($P2_1/m$, #11, $Z = 2$) were synthesized at pressures of 39(2) and 45(2) GPa, respectively. The unit cell of $Gd_{19}ClC_{18}$ comprises 11 crystallographically distinct metal atoms (8 of them at the 4*f* and three at the 2*e* Wyckoff positions), 10 distinct carbon atoms (8 at the 4*f* site form dumbbells, whereas the other two at the 2*e* site are not catenated), and one chlorine atom at the 2*e* Wyckoff site (Table S6). Metal atoms are surrounded by carbon and chlorine atoms forming various irregular polyhedra with coordination numbers of 6, 7, or 8. Figure 4b presents the polyhedral model, as viewed along the *a* (left) and *b* (right) directions. The interatomic distances are presented in Supplementary Table S6. The structure of the samarium compound exhibits a pronounced residual electron density peak located 0.704(9) Å from Sm11, which may be attributed to positional disorder of the samarium atom. In the initial refinement, the model displayed a chemically unreasonable Sm12−Cl1 distance and a relatively high atomic displacement parameter (ADP) for the chlorine atom. Subsequent refinements of the occupancies for the Sm11, Sm12, and Cl1 sites markedly improved the structural model (Table S6). The results indicate that, in a part of the structure, samarium occupies the Sm11 position with chlorine present at the Cl1 site, whereas in the remaining fraction, samarium is located at the Sm12 position with no chlorine in its first coordination sphere.

The novel samarium and gadolinium chloride carbides contain carbon in the form of discrete atoms and dumbbells. Assuming that the metal atoms have an oxidation state of 3+, the charge distribution can be represented as $REE^{3+}{}_{19}Cl^{-}[C_2]^{6-}{}_8C^{4-}{}_2$. The assumed formal charges suggest a single-bond character in the $[C_2]$ dumbbells.

**Dysprosium Chloride Carbide.** The novel dysprosium chloride carbide *hP*18 $Dy_5Cl_3C$ crystallized at 122(3) GPa. Having a hexagonal symmetry (space group $P6_3/mcm$, #193, $Z = 2$) (Figure 4c, Table S7), it adopts the $Cr_5Si_3B$-type[43] structure known for B-, C-, N-, and O-containing ternary compounds $M_5X_3L_x$ (L = B, C, N, O, Cl, Br, or I, $x \leq 1$), where M is a metal (REE, Ti, Zr, Hf, V, Nb, Ta, Cr, Mo, or Mn) and X is typically Zn, Cd, Al, Ga, In, Tl, Si, Ge, Ga, Sn, As, Sb, or Bi.[44−52] This structure type is a derivative of the $Ga_4Ti_5$ structure type (the CCDC deposition number 103997).[53] The latter was recently reported for novel


https://doi.org/10.1021/acsomega.5c09373
ACS Omega 2026, 11, 4280−4289

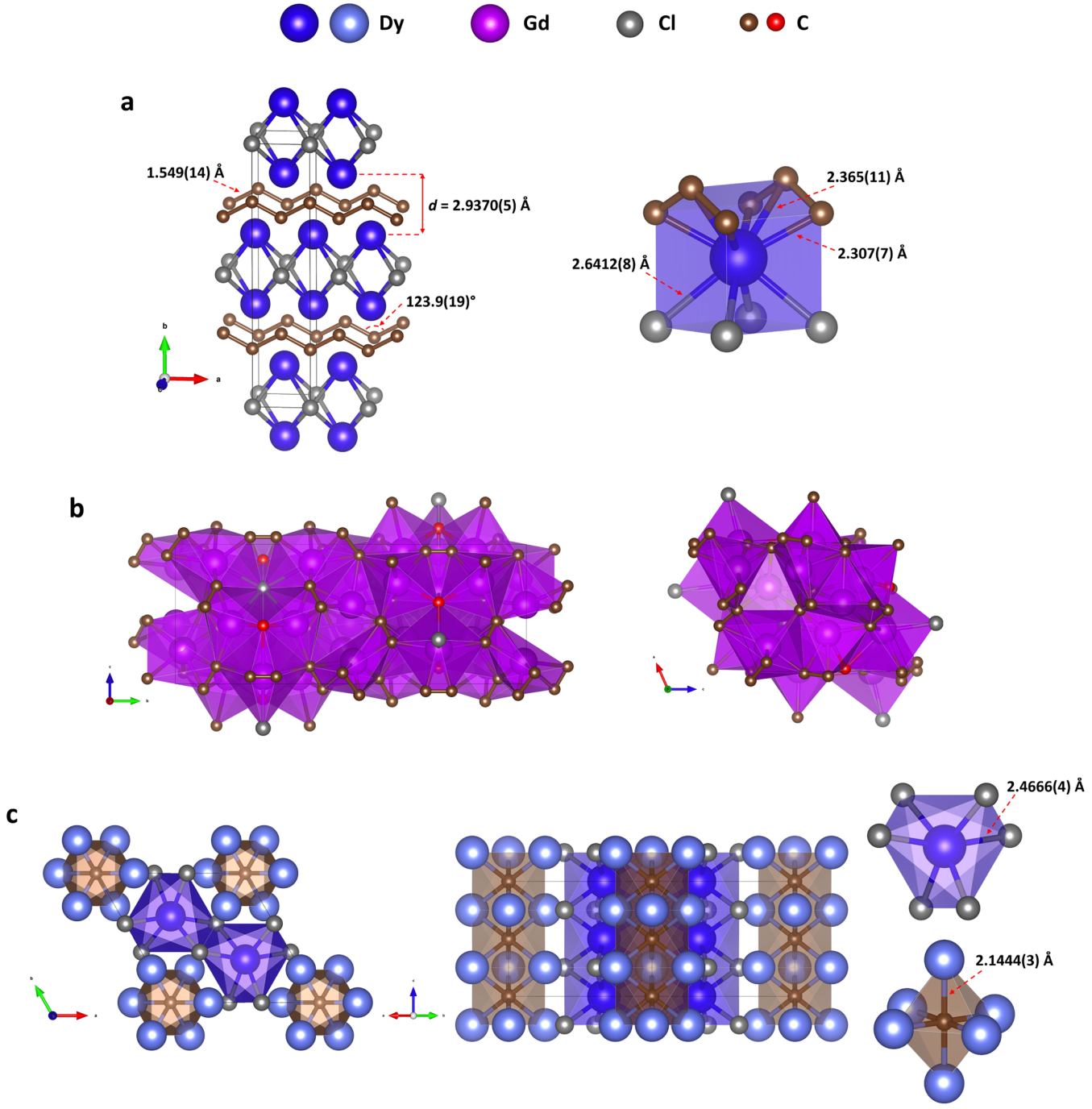


**Figure 4.** Crystal structures of rare-earth metal chloride carbides *o*C10 $Dy_2ClC_2$ (and isostructural $Gd_2ClC_2$ and $Sm_2ClC_2$), *m*P76 $Gd_{19}ClC_{18}$ (and isostructural $Sm_{19}ClC_{18}$), and *h*P18 $Dy_5Cl_3C$. (a) *o*C10 $Dy_2ClC_2$ at 76(3) GPa: stick-and-ball model (left) and coordination of Dy atoms (right). (b) *m*P76 $Gd_{19}ClC_{18}$ at 45(2) GPa: polyhedral model as viewed along the *a* (left) and *b* (right) directions. (c) *h*P18 $Dy_5Cl_3C$ at 122(3) GPa; from left to right: polyhedral model viewed along the *c* axis and [110] direction; $C(Dy2)_6$ octahedron; $Dy1Cl_6$ twisted trigonal prism. Dysprosium atoms in two crystallographically distinct positions are shown with different colors: Dy1—dark blue, Dy2—light blue; Gd—purple; Cl—gray; C catenated—brown; discrete C atoms—red.

isostructural sodium polychloride *h*P18-$Na_4Cl_5$ and sodium polybromide *h*P18-$Na_4Br_5$.[54]

In the structure of *h*P18 $Dy_5Cl_3C$, C and Cl are at the 2*b* and 6*g* Wyckoff sites, and Dy1 and Dy2 are at the 4*d* and 6*g*, respectively. Geometrically, Dy1 atoms form linear chains aligned along the *c* direction with a Dy1−Dy1 distance of 2.4188(7) Å. C atoms also form linear chains along the *c* direction with a C−C distance of 2.4188(7) Å (Figure 4c). C atoms are coordinated by six Dy2 atoms, forming an octahedron with an edge length of 2.9978(5) or 3.0672(3) Å. Dy1 atoms have a twisted trigonal prismatic coordination by the six nearest equidistant chlorine atoms with *d*(Dy1−Cl1) = 2.4666(4) Å (at the synthesis pressure). Thus, the structure of *h*P18 $Dy_5Cl_3C$ is easily visualized as being formed by two distinct columnar arrangements in the *c* direction, those of face-sharing $C(Dy2)_6$ octahedra and face-sharing $Dy1Cl_6$ twisted trigonal prism (see the polyhedral model viewed along the *c* and [110] directions in Figure 4c).



https://doi.org/10.1021/acsomega.5c09373
ACS Omega 2026, 11, 4280−4289

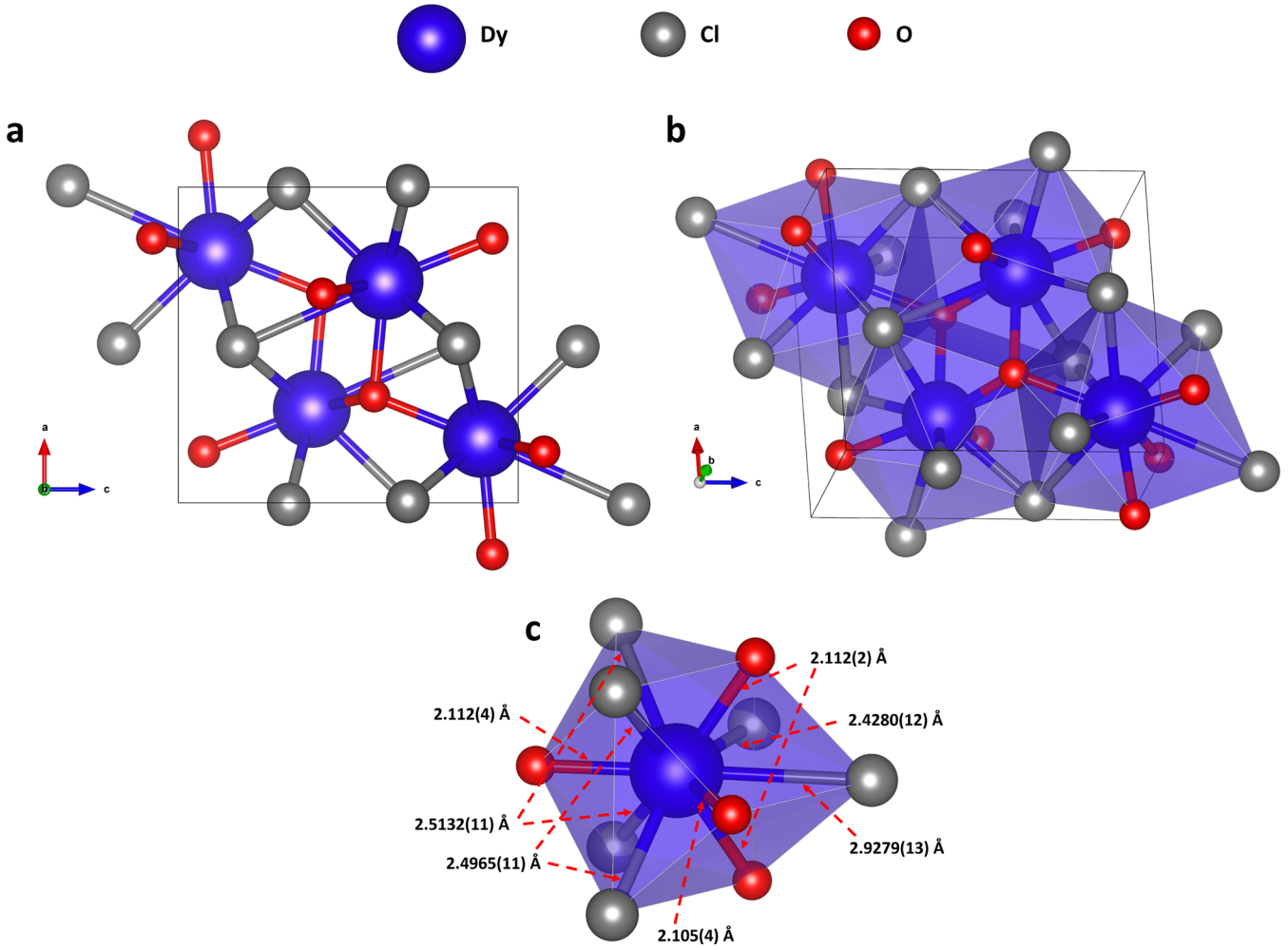


**Figure 5.** Crystal structure of *oP*12 DyOCl at 108(3) GPa. (a) Stick-and-ball model projected along the *a* axis. (b) Perspective view of the polyhedral model. (c) Coordination of Dy atoms. Dysprosium atoms are blue, oxygen is red, and chlorine is gray.

**Structure of Dysprosium Oxychloride.** The previously unknown modification of dysprosium oxide chloride *oP*12 DyOCl (space group *Pnma*, #62, $Z = 4$) (Figure 5, Table S8) with the TiNiSi-type[55] (or SrMgSi-type[56]) structure was synthesized in the current work at 76(3) and 108(3) GPa. The novel compound differs from the previously reported *tP*6 DyOCl[57,58] (PbFCl-type structure, space group *P*4/*nmm*, #129, $Z = 2$). In the structure of *oP*12 DyOCl, dysprosium, oxygen, and chlorine atoms occupy the Wyckoff position 4*c*. Four oxygen and six chlorine atoms coordinate Dy atoms forming a bicapped tetragonal antiprism, which share both triangular and square faces (Figure 5b, c). The interatomic distances at 108(3) GPa are $d$(Dy−O) = 2.105(4)−2.112(4) Å and $d$(Dy−Cl) = 2.4280(12)−2.9279(13) Å (Figure 5c).

## DISCUSSION

Alkali halides, especially sodium chloride, are known for their chemical inertness in the solid form. Due to this, in HPHT experiments, they have been used as inert pressure-transmitting media,[59] electrical and thermal insulators,[59−61] and pressure calibrants.[20,62] However, recent advances in both experimental and theoretical investigations have shed light on the unusual behavior of the Na−Cl system under high pressure, revealing the formation of several compounds with atypical stoichiometry, such as $Na_4Cl_5$ and $Na_2Cl_3$,[54] for example. It was found that NaCl used as a pressure-transmitting medium in experiments with REEs reacts not only with metals but also with carbon from diamond anvils, leading to the formation of not only metal chlorides, such as $Y_2Cl$ and DyCl, but also chloride carbides, $Y_2ClC$ and $Dy_2ClC$.[4]

In the course of this work, we have demonstrated that the synthesis of new binary and ternary Cl-bearing compounds from metals and NaCl (plus C and O) can be carried out deliberately and reproducibly. Twelve new compounds have been synthesized: *tI*6 $La_2Cl$, *oC*8 LaCl, *oP*8 $LaCl_3$, *cP*2 DyCl, *oI*32 $DyNa_2Cl_5$, *oC*10 $Sm_2ClC_2$, *oC*10 $Gd_2ClC_2$, *oC*10 $Dy_2ClC_2$, *mP*76 $Sm_{19}ClC_{18}$, *mP*76 $Gd_{19}ClC_{18}$, *hP*18 $Dy_5Cl_3C$, and *oP*12 DyOCl. All of them, except one (*mP*76 $Sm_{19}ClC_{18}$), crystallize in known structural types ($MoSi_2$, TlI (B33, *Cmcm*), $Cu_3Ti$, CsCl, $NH_4Pb_2Br_5$, $Mn_2AlB_2$, $Cr_5Si_3B$, and TiNiSi). However, many questions regarding the peculiarities of the chemical processes remain open. For example, we observed Na-containing compounds upon heating Dy in NaCl—*hP*18 $Na_4Cl_5$[54] at 95 GPa (Tables S1 and S9) and *oI*32 $DyNa_2Cl_5$ at 107(3) GPa (Tables S1 and S4)—in a single experiment. What happened with Na in other experiments is unclear. We can speculate that Na-containing compounds may be amorphous or decompose upon temperature quenching, but resolving this issue requires further *in situ* HPHT experiments.



https://doi.org/10.1021/acsomega.5c09373
ACS Omega 2026, 11, 4280−4289

The design of an experiment, especially the position of a sample in the pressure chamber, may affect its outcome, and under similar PT conditions, the predominant reaction products may be different. However, a definite conclusion, whether direct contact of metal with the diamond (Figure 1a) facilitates the synthesis of carbides, whereas isolation of metal from anvils by the pressure medium (NaCl) (Figure 1b) stimulates the synthesis of Cl-containing compounds, cannot yet be made. In all experiments in this work and our previous studies,[63,64] a piece of metal was placed directly on the diamond culet (Figure 1a); however, at 19−70 GPa in refs 63 and 64, the primary products were carbides, such as $\gamma$-$DyC_2$, $Dy_5C_9$, $Dy_2C_3$, $\gamma$-$Dy_4C_5$, $Dy_4C_3$, and $Dy_3C_2$, whereas in the present work at similar PT conditions, both chlorides and chloride carbides were synthesized. In ref. 4, at 40 GPa with the experimental design according to Figure 1b, the main products were DyCl and the chloride carbide $Dy_2ClC$.[4]

It would be interesting to see whether there is a correlation between the atomic radii of the REEs and their reactivity with NaCl (Figure S1). Sc pressurized and heated in NaCl at 64 GPa formed only $Sc_4C_3$ carbide known at ambient conditions.[65] In contrast, heating Sm in NaCl at 62 GPa resulted in the synthesis of both novel carbides and a chloride carbide, $Sm_2ClC_2$ (Table S1). Dy seems to be the most reactive compared to all other studied REEs, but it is not clear if this relates to its enhanced reactivity, more studies conducted, or the particular design of the experiments. More studies are needed to clarify this point.

The formation of zigzag (*trans*-polyacetylene-like) carbon chains was previously suggested for the Li−C and Ca−C systems[66−68] but has never been observed. In this study, such chains were identified for the first time in a series of isostructural lanthanide (Dy, Gd, and Sm) chloride carbides, *o*C10 $Dy_2ClC_2$, $Gd_2ClC_2$, and $Sm_2ClC_2$, with an *o*C10 $Mn_2AlB_2$-type structure (Figure 4a). Interestingly, the structure of these chloride carbides is very similar to that of *tI*6 $La_2Cl$ (Figure 2a). Both the former and the latter are built of layers of edge-sharing unoccupied metal−chlorine $Me_2Cl_4$ octahedra stacking one upon another. However, in the chloride carbides, these layers alternate with the layers of zigzag carbon chains (Figure 4a). Notably, there is another polymorph of a rare-earth metal chloride with the same stoichiometry, *tI*12 $Y_2Cl$[4], which adopts a different structure.

Considering the interatomic distances in *o*C10 $Dy_2ClC_2$ at 76(3) GPa, metal atoms are coordinated by four nearest chlorine ($d$(Dy−Cl) = 2.6412(8) Å) and six nearest carbon atoms ($d$(Dy−C) = 2.307(7) or 2.365(11) Å) (Figure 4a, right)—the latter being shorter than $d$(Dy−C) in $\gamma$-$DyC_2$ ($d$(Dy−C) ∼ 2.43 Å) and $Dy_4C_3$ ($d$(Dy−C) ∼ 2.39 Å) at similar pressures (according to the EoSs in ref 64). It seems common that the presence of chlorine anions in the structure results in a shortening of the metal−carbon distances in chloride carbides. For example, in the aforementioned *hP*18 $Dy_5Cl_3C$ $d$(Dy−C) = 2.1444(3) Å, which is also shorter than in $Dy_4C_3$ ($d$(Dy−C) ∼ 2.26 Å—as expected based on the EoS[64]). This observation can be attributed to charge redistribution in the synthesized ternary metal−chlorine−carbon compounds. The highly electronegative chlorine withdraws electron density from the metal atoms, increasing their positive charge and strengthening their interaction with carbon.

## CONCLUSION

To summarize, the chemical reactions between NaCl and La, Sm, Gd, or Dy, observed in this work upon laser heating of the metals to 2500−2800 K at 39−127 GPa in DACs, resulted in the synthesis of previously unknown chlorides ($La_2Cl$, LaCl, $LaCl_3$, and DyCl), chloride carbides ($Sm_2ClC_2$, $Gd_2ClC_2$, $Dy_2ClC_2$, $Sm_{19}ClC_{18}$, $Gd_{19}ClC_{18}$, $Dy_5Cl_3C$), an oxide chloride (DyOCl), and a ternary chloride ($DyNa_2Cl_5$). The latter is the first observation of a ternary Na-containing compound as a product of the HPHT reaction with NaCl. For the first time, zigzag (*trans*-polyacetylene-like) carbon chains have been identified in *o*C10 $Mn_2AlB_2$-type lanthanide chloride carbides. Additionally, it was demonstrated that the presence of chlorine atoms shortens metal−carbon distances in lanthanide chloride carbides compared to previously reported carbides.[64] These findings enhance our understanding of chemical bonding in ternary rare-earth compounds under high pressure, paving the way for further studies of their crystal chemistry under extreme conditions.

Our methodology for the synthesis of novel chlorides and chloride carbides by the direct reaction of metals with halides at high pressure and temperature in laser-heated DACs results in producing phase mixtures. Although the individual phases cannot yet be separated, our approach allows investigating "pressure−temperature-phase-structure" space and significantly expands our knowledge of materials that can be synthesized under certain PT conditions.

## ASSOCIATED CONTENT

### Supporting Information

The Supporting Information is available free of charge at https://pubs.acs.org/doi/10.1021/acsomega.5c09373.

Summary of the performed DAC laser heating experiments and crystallographic information (PDF)

### Accession Codes

CCDC 2477205−2477220 contain the supplementary crystallographic data for this paper. These data can be obtained free of charge from The Cambridge Crystallographic Data Centre via www.ccdc.cam.ac.uk/data_request/cif.

## AUTHOR INFORMATION


### Corresponding Authors

**Fariia Iasmin Akbar** − *Institute of Inorganic and Analytical Chemistry, Goethe University Frankfurt, Frankfurt 60438, Germany; Bavarian Research Institute of Experimental Geochemistry and Geophysics (BGI), University of Bayreuth, Bayreuth 95440, Germany;* orcid.org/0000-0002-6016-5849; Email: akbar@chemie.uni-frankfurt.de

**Leonid Dubrovinsky** − *Bavarian Research Institute of Experimental Geochemistry and Geophysics (BGI), University of Bayreuth, Bayreuth 95440, Germany;* Email: Leonid.Dubrovinsky@uni-bayreuth.de

### Authors

**Alena Aslandukova** − *Institute of Inorganic and Analytical Chemistry, Goethe University Frankfurt, Frankfurt 60438, Germany; Bavarian Research Institute of Experimental Geochemistry and Geophysics (BGI), University of Bayreuth, Bayreuth 95440, Germany*

**Andrey Aslandukov** − *Institute of Inorganic and Analytical Chemistry, Goethe University Frankfurt, Frankfurt 60438,*




https://doi.org/10.1021/acsomega.5c09373
ACS Omega 2026, 11, 4280−4289

*Germany; Material Physics and Technology at Extreme Conditions, Bavarian Research Institute of Experimental Geochemistry and Geophysics (BGI), University of Bayreuth, Bayreuth 95440, Germany;* orcid.org/0000-0003-0988-6066

**Yuqing Yin** − *Bavarian Research Institute of Experimental Geochemistry and Geophysics (BGI), University of Bayreuth, Bayreuth 95440, Germany; Department of Physics, Chemistry and Biology (IFM), Linköping University, Linköping SE-581 83, Sweden;* orcid.org/0000-0001-8861-8443

**Elena Bykova** − *Institute of Geosciences, Goethe University Frankfurt, Frankfurt am Main 60438, Germany*

**Maxim Bykov** − *Institute of Inorganic and Analytical Chemistry, Goethe University Frankfurt, Frankfurt 60438, Germany;* orcid.org/0000-0003-0248-1728

**Dominique Laniel** − *Centre for Science at Extreme Conditions and School of Physics and Astronomy, University of Edinburgh, Edinburgh EH9 3FD, United Kingdom*

**Pavel Milkin** − *Faculty of Engineering Sciences, University of Bayreuth, Bayreuth 95447, Germany*

**Timofey Fedotenko** − *Deutsches Elektronen-Synchrotron DESY, Hamburg 22607, Germany*

**Jonathan Wright** − *European Synchrotron Radiation Facility, Grenoble 38043, France*

**Anna Pakhomova** − *European Synchrotron Radiation Facility, Grenoble 38043, France*

**Gaston Garbarino** − *European Synchrotron Radiation Facility, Grenoble 38043, France*

**Mohamed Mezouar** − *European Synchrotron Radiation Facility, Grenoble 38043, France;* orcid.org/0000-0001-5336-544X

**Michael Hanfland** − *European Synchrotron Radiation Facility, Grenoble 38043, France*

**Natalia Dubrovinskaia** − *Material Physics and Technology at Extreme Conditions, Bavarian Research Institute of Experimental Geochemistry and Geophysics (BGI), University of Bayreuth, Bayreuth 95440, Germany;* orcid.org/0000-0002-8256-5675

Complete contact information is available at: https://pubs.acs.org/10.1021/acsomega.5c09373

## Notes

The authors declare no competing financial interest.

## ■ ACKNOWLEDGMENTS

The authors acknowledge the Deutsches Elektronen-Synchrotron (DESY, PETRA III) for the provision of beamtime at the P02.2 beamline (with thanks to Dr. Hanns-Peter Liermann for maintaining the beamline infrastructure), and the European Synchrotron Radiation Facility for the provision of beamtime at the ID11, ID15b, and ID27 beamlines (experiments: HC-5074,[69] HC-5082,[70] HC-4883,[71] CH-6473,[72] CH-6542,[73] CH-6544,[74] CH-6627,[75] HC-5588[76]). N.D. thanks the Deutsche Forschungsgemeinschaft (DU 945/15-1) for financial support. D.L. thanks the UKRI Future Leaders Fellowship (MR/V025724/1) for financial support. For the purpose of open access, the author has applied a Creative Commons Attribution (CC BY) license to any Author Accepted Manuscript version arising from this submission.

## ■ REFERENCES

(1) Lhoste, J.; Henry, N.; Loiseau, T.; Abraham, F. Microwave-Assisted Synthesis of a Neodymium Trichloride Complex with Phenanthroline Containing Infinite Chains, NdCl3(H2O)(Phen). *Inorg. Chem. Commun.* **2011**, *14* (9), 1525−1527.

(2) Habashi, F. Extractive Metallurgy of Rare Earths. *Can. Metall. Q.* **2013**, *52* (3), 224−233.

(3) Kwag, G.; Kim, D.; Lee, S.; Bae, C. Morphology and Activity of Nanosized NdCl3 Catalyst for 1,3-butadiene Polymerization. *J. Appl. Polym. Sci.* **2005**, *97* (3), 1279−1283.

(4) Yin, Y.; Akbar, F. I.; Bykova, E.; Aslandukova, A.; Laniel, D.; Aslandukov, A.; Bykov, M.; Hanfland, M.; Garbarino, G.; Jia, Z.; Dubrovinsky, L.; Dubrovinskaia, N. Synthesis of Rare-Earth Metal Compounds through Enhanced Reactivity of Alkali Halides at High Pressures. *Commun. Chem.* **2022**, *5* (1), 8−13.

(5) Bai, X.; Xue, Y.; Luo, K.; Chen, K.; Huang, Q.; Zha, X.-H.; Du, S. Two-Dimensional Half-Metallic and Semiconducting Lanthanide-Based MXenes. *ACS Omega* **2022**, *7*, 40929.

(6) Yin, Y.-C.; Yang, J.-T.; Luo, J.-D.; Lu, G.-X.; Huang, Z.; Wang, J.-P.; Li, P.; Li, F.; Wu, Y.-C.; Tian, T.; Meng, Y.-F.; Mo, H.-S.; Song, Y.-H.; Yang, J.-N.; Feng, L.-Z.; Ma, T.; Wen, W.; Gong, K.; Wang, L.-J.; Ju, H.-X.; Xiao, Y.; Li, Z.; Tao, X.; Yao, H.-B. A LaCl3-Based Lithium Superionic Conductor Compatible with Lithium Metal. *Nature* **2023**, *616* (7955), 77−83.

(7) Ahn, K.; Gibson, B. J.; Kremer, R. K.; Mattausch, H.; Stolovits, A.; Simon, A. The Layered Lanthanum Carbide Halide Superconductors La2C2(XX‘)2 (X,X‘= Cl, Br, I): Neutron Powder Diffraction Characterization and Electronic Properties. *J. Phys. Chem. B* **1999**, *103* (26), 5446−5453.

(8) Chiba, T.; Sato, J.; Ishikawa, S.; Takahashi, Y.; Ebe, H.; Sumikoshi, S.; Ohisa, S.; Kido, J. Neodymium Chloride-Doped Perovskite Nanocrystals for Efficient Blue Light-Emitting Devices. *ACS Appl. Mater. Interfaces* **2020**, *12* (48), 53891−53898.

(9) Marsden, K. C.; Pesic, B. Evaluation of the Electrochemical Behavior of CeCl3 in Molten LiCl-KCl Eutectic Utilizing Metallic Ce as an Anode. *J. Electrochem. Soc.* **2011**, *158* (6), F111.

(10) Xi, X.; Wang, J.; Zhang, J.; Li, W.; Ning, S.; Jiang, T.; Wei, Y.; Han, W. Electrochemical Behavior and Separation of Ce(III) in LiCl-KCl Molten Salt. *Sep. Purif. Technol.* **2024**, *334*, 125931.

(11) Peringer, E.; Tejuja, C.; Salzinger, M.; Lemonidou, A. A.; Lercher, J. A. On the Synthesis of LaCl3 Catalysts for Oxidative Chlorination of Methane. *Appl. Catal. A* **2008**, *350* (2), 178−185.

(12) Ismail, M.; Mustafa, N. S.; Juahir, N.; Yap, F. A. H. Catalytic Effect of CeCl3 on the Hydrogen Storage Properties of MgH2. *Mater. Chem. Phys.* **2016**, *170*, 77−82.

(13) Pomiro, F. J.; Gaviría, J. P.; Fouga, G. G.; Bohé, A. E.; De Micco, G. A Panoramic Overview of Chlorination and Carbochlorination of Light Rare Earth Oxides, Including Thermodynamic, Reaction Mechanism, and Kinetic Aspects. *Min., Metall., Explor.* **2021**, *38* (6), 2467−2484.

(14) Mattausch, H.; Schaloske, M. C.; Hoch, C.; Simon, A. Halogenide der Seltenerdmetalle Ln 4 X 5 Z. Teil 2: Eine orthorhombische Verknüpfungsvariante o -Ln 4 X 5 Z. *Z. Anorg. Allg. Chem.* **2008**, *634* (3), 498−502.

(15) Simon, A.; Schwarz, C.; Bauhofer, W. Ein Neues Lanthanoidcarbidhalogenid, Gd6Cl5C3. *J. Less Common Met.* **1988**, *137* (1−2), 343−351.

(16) Hwu, S. J.; Ziebarth, R. P.; Von Winbush, S.; Ford, J. E.; Corbett, J. D. Synthesis and Structure of Double-Metal-Layered Scandium, Yttrium, and Zirconium Chloride Carbides and Nitrides, M2Cl2C and M2Cl2N. *Inorg. Chem.* **1986**, *25* (3), 283−287.

(17) Teplonogova, M. A.; Kozlova, A. A.; Yapryntsev, A. D.; Baranchikov, A. E.; Ivanov, V. K. Synthesis and Thermal Decomposition of High-Entropy Layered Rare Earth Hydroxychlorides. *Molecules* **2024**, *29* (7), 1634.

(18) Kantor, I.; Prakapenka, V.; Kantor, A.; Dera, P.; Kurnosov, A.; Sinogeikin, S.; Dubrovinskaia, N.; Dubrovinsky, L. BX90: A New Diamond Anvil Cell Design for X-Ray Diffraction and Optical Measurements. *Rev. Sci. Instrum.* **2012**, *83* (12), 125102.

(19) Fedotenko, T.; Dubrovinsky, L.; Aprilis, G.; Koemets, E.; Snigirev, A.; Snigireva, I.; Barannikov, A.; Ershov, P.; Cova, F.; Hanfland, M.; Dubrovinskaia, N. Laser Heating Setup for Diamond Anvil Cells for in Situ Synchrotron and in House High and Ultra-High Pressure Studies. *Rev. Sci. Instrum.* **2019**, *90* (10), 104501.
(20) Dorogokupets, P. I.; Dewaele, A. Equations of State of MgO, Au, Pt, NaCl-B1, and NaCl-B2: Internally Consistent High-Temperature Pressure Scales. *High Pressure Res.* **2007**, *27* (4), 431−446.
(21) Sakai, T.; Ohtani, E.; Hirao, N.; Ohishi, Y. Equation of State of the NaCl-B2 Phase up to 304 GPa. *J. Appl. Phys.* **2011**, *109* (8), 084912.
(22) Hrubiak, R.; Smith, J. S.; Shen, G. Multimode Scanning X-Ray Diffraction Microscopy for Diamond Anvil Cell Experiments. *Rev. Sci. Instrum.* **2019**, *90* (2), 025109.
(23) *Rigaku Oxford Diffraction*; CrysAlisPro Software System, 2015.
(24) Aslandukov, A.; Aslandukov, M.; Dubrovinskaia, N.; Dubrovinsky, L. *Domain Auto Finder* (*DAFi*) Program: The Analysis of Single-Crystal X-Ray Diffraction Data from Polycrystalline Samples. *J. Appl. Crystallogr.* **2022**, *55*, 1383−1391.
(25) Dolomanov, O. V.; Bourhis, L. J.; Gildea, R. J.; Howard, J. A. K.; Puschmann, H. *OLEX2*: A Complete Structure Solution, Refinement and Analysis Program. *J. Appl. Crystallogr.* **2009**, *42* (2), 339−341.
(26) Sheldrick, G. M. *SHELXT* − Integrated Space-Group and Crystal-Structure Determination. *Acta Crystallogr.* **2015**, *A71* (1), 3−8.
(27) Sheldrick, G. M. Crystal Structure Refinement with *SHELXL*. *Acta Crystallogr.* **2015**, *C71* (1), 3−8.
(28) Momma, K.; Izumi, F. *VESTA 3* for Three-Dimensional Visualization of Crystal, Volumetric and Morphology Data. *J. Appl. Crystallogr.* **2011**, *44* (6), 1272−1276.
(29) Link, L.; Niewa, R. Polynator: A Tool to Identify and Quantitatively Evaluate Polyhedra and Other Shapes in Crystal Structures. *J. Appl. Crystallogr.* **2023**, *56* (6), 1855−1864.
(30) Beck, H. P.; Schuster, M. High-Pressure Transformations of NdI2. *J. Solid State Chem.* **1992**, *100* (2), 301−306.
(31) Burrow, J. H.; Maule, C. H.; Strange, P.; Tothill, J. N.; Wilson, J. A. The Electronic Conditions in the 5d1 Layer-Metal LaI2Making Comparison with the Iso-Electronic Tantalum Dichalcogenides, with the Other RE Di-Iodides, and with the RE Monochalcogenides. *J. Phys. C* **1987**, *20* (26), 4115−4133.
(32) Inorganic Crystal Structure Database; *Version 5.4.0 (build 20250403−0947)- Data Release 2025.1*. https://icsd.fiz-karlsruhe.de/search/basic.xhtml.
(33) Yu, H.; Chen, Y. Pressure-Induced Electrides and Metallic Phases in the Y−Cl System. *J. Phys.: Condens. Matter* **2021**, *33* (21), 215401.
(34) Chattopadhyay, T.; Werner, A.; von Schnering, H. G.; Pannetier, J. Temperature and Pressure Induced Phase Transition in IV-VI Compounds. *Rev. Phys. Appl.* **1984**, *19* (9), 807−813.
(35) Araujo, R. E.; Corbett, J. D. Lanthanum Monochloride and Lanthanum Sesquichloride. *Inorg. Chem.* **1981**, *20* (9), 3082−3086.
(36) Morosin, B. Crystal Structures of Anhydrous Rare-Earth Chlorides. *J. Chem. Phys.* **1968**, *49* (7), 3007−3012.
(37) Crichton, W. A.; Bouvier, P.; Winkler, B.; Grzechnik, A. The Structural Behaviour of LaF3 at High Pressures. *Dalton Trans.* **2010**, *39* (18), 4302.
(38) Powell, H. M.; Tasker, H. S. The Valency Angle of Bivalent Lead: The Crystal Structure of Ammonium, Rubidium, and Potassium Pentabromodiplumbites. *J. Chem. Soc.* **1937**, 119−123.
(39) Abrahams, I.; Demetriou, D. Z.; Kroemer, R. T.; Taylor, H.; Motevalli, M. Evidence for Cluster Orbital Formation in CsSn2 × 5 Compounds (X = Cl, Br). *J. Solid State Chem.* **2001**, *160* (2), 382−387.
(40) Beck, H. P.; Clicqué, G.; Nau, H. A Study on AB2 × 5 Compounds (A: K, In, Tl; B: Sr, Sn, Pb; X: Cl, Br, I). *Z. Anorg. Allg. Chem.* **1986**, *536* (5), 35−44.
(41) Ade, M.; Hillebrecht, H. Ternary Borides Cr2AlB2, Cr3AlB4, and Cr4AlB6: The First Members of the Series (CrB2)NCrAl with n = 1, 2, 3 and a Unifying Concept for Ternary Borides as MAB-Phases. *Inorg. Chem.* **2015**, *54* (13), 6122−6135.
(42) Ali, T.; Khan, M. N.; Ahmed, E.; Ali, A. Phase Analysis of AlFe2B2 by Synchrotron X-Ray Diffraction, Magnetic and Mössbauer Studies. *Prog. Nat. Sci.: Mater. Int.* **2017**, *27* (2), 251−256.
(43) Nowotny, H.; Piegger, E.; Kieffer, R.; Benesovsky, F. Das Dreistoffsystem: Chrom-Silizium-Bor. *Monatsh. Chem.* **1958**, *89* (4−5), 611−617.
(44) Jeitschko, W.; Nowotny, H.; Benesovsky, F. Verbindungen Vom Typ T5M3X. *Monatsh. Chem.* **1964**, *95* (4−5), 1242−1246.
(45) Yamane, H.; Amano, S. Ternary Suboxides Ti7Ga2O6, Ti3GaO, and Ti5Ga3O. *Inorg. Chem.* **2018**, *57* (16), 9941−9948.
(46) Mayer, I.; Felner, I. Nowotny Phases of M5 × 3-Type Rare-Earth Silicides and Germanides with Boron. *J. Less Common Met.* **1974**, *37* (1), 171−173.
(47) Roger, J.; Ben Yahia, M.; Babizhetskyy, V.; Bauer, J.; Cordier, S.; Guérin, R.; Hiebl, K.; Rocquefelte, X.; Saillard, J.-Y.; Halet, J.-F. Mn5Si3-Type Host-Interstitial Boron Rare-Earth Metal Silicide Compounds RE5Si3: Crystal Structures, Physical Properties and Theoretical Considerations. *J. Solid State Chem.* **2006**, *179* (8), 2310−2328.
(48) Kwon, Y. U.; Corbett, J. D. Chemistry in Polar Intermetallic Compounds. The Interstitial Chemistry of Zirconium-Tin (Zr5Sn3). *Chem. Mater.* **1992**, *4* (6), 1348−1355.
(49) Kim, S.-J.; Kematick, R. J.; Yi, S. S.; Franzen, H. F. On the Stabilization of Zr5Al3 in the Mn5Si3-Type Structure by Interstitial Oxygen. *J. Less Common Met.* **1988**, *137* (1−2), 55−59.
(50) Holleck, H.; Rieger, W.; Nowotny, H.; Benesovsky, F. Die Phasen Nb3Ga2, Ta5Ga3 Und Ta5Al3Bx. *Monatsh. Chem.* **1964**, *95* (2), 552−557.
(51) Zheng, C.; Mattausch, H.; Simon, A. La5M3X (M = Sn, Bi; X = Cl, Br, I): Exploring the Limit of the Mn5Si3-Type Hosting Lattice. *J. Alloys Compd.* **2002**, *347* (1−2), 79−85.
(52) Jensen, E. A.; Hoistad, L. M.; Corbett, J. D. Lanthanum and Praseodymium Bromide Pnictides. A Convergence of Interstitial Chemistry in Cluster Halides and Intermetallic Pnictides. *J. Solid State Chem.* **1999**, *144* (1), 175−180.
(53) Schubert, K.; Meissner, H. G.; Pötzschke, M.; Rossteutscher, W.; Stolz, E. Einige Strukturdaten Metallischer Phasen (7). *Naturwissenschaften* **1962**, *49* (3), 57.
(54) Yin, Y.; Aslandukova, A.; Jena, N.; Trybel, F.; Abrikosov, I. A.; Winkler, B.; Khandarkhaeva, S.; Fedotenko, T.; Bykova, E.; Laniel, D.; Bykov, M.; Aslandukov, A.; Akbar, F. I.; Glazyrin, K.; Garbarino, G.; Giacobbe, C.; Bright, E. L.; Jia, Z.; Dubrovinsky, L.; Dubrovinskaia, N. Unraveling the Bonding Complexity of Polyhalogen Anions: High-Pressure Synthesis of Unpredicted Sodium Chlorides Na2Cl3 and Na4Cl5 and Bromide Na4Br5. *JACS Au* **2023**, *3* (6), 1634−1641.
(55) Landrum, G. A.; Hoffmann, R.; Evers, J.; Boysen, H. The TiNiSi Family of Compounds: Structure and Bonding. *Inorg. Chem.* **1998**, *37* (22), 5754−5763.
(56) Eisenmann, B.; Schäfer, H.; Weiss, A. Der Übergang Vom "geordneten" Anti-PbCl2 -Gitter Zum Anti-PbFCl-Gitter: Ternäre Phasen ABX Der Erdalkalimetalle Mit Elementen Der 4. Hauptgruppe (A = Ca, Sr, Ba; B = Mg; X = Si, Ge, Sn, Pb). *Z. Anorg. Allg. Chem.* **1972**, *391* (3), 241−254.
(57) Tian, C.; Pan, F.; Wang, L.; Ye, D.; Sheng, J.; Wang, J.; Liu, J.; Huang, J.; Zhang, H.; Xu, D.; Qin, J.; Hao, L.; Xia, Y.; Li, H.; Tong, X.; Wu, L.; Chen, J.-H.; Jia, S.; Cheng, P.; Yang, J.; Zheng, Y. DyOCl: A Rare-Earth Based Two-Dimensional van Der Waals Material with Strong Magnetic Anisotropy. *Phys. Rev. B* **2021**, *104* (21), 214410.
(58) Chong, S.; Riley, B. J.; Marcial, J.; Lonergan, C. E.; Cutforth, D. A. Synthesis of Dysprosium Oxychloride (DyOCl). *J. Chem. Crystallogr.* **2022**, *52* (2), 185−193.
(59) Hu, J.; Xu, J.; Somayazulu, M.; Guo, Q.; Hemley, R.; Mao, H. K. X-Ray Diffraction and Laser Heating: Application of a Moissanite Anvil Cell. *J. Phys.: Condens. Matter* **2002**, *14* (44), 10479−10481.
(60) Armentrout, M.; Kavner, A. High Pressure High Temperature Equation of State for Fe2SiO4 Ringwoodite and Implications for the Earth's Transition Zone. *Geophys. Res. Lett.* **2011**, *38* (8), 1−4.


https://doi.org/10.1021/acsomega.5c09373
*ACS Omega* 2026, 11, 4280−4289

(61) Langerome, B.; Verseils, M.; Capitani, F.; Brubach, J. B.; Amzallag, E.; Calandrini, E.; Creuze, J.; Roy, P. Probing NaCl at High Pressure through Optical Studies and Ab Initio Calculations. *J. Phys. Chem. C* **2019**, *123* (25), 15724−15728.
(62) Decker, D. L. Equation of State of NaCl and Its Use as a Pressure Gauge in High-Pressure Research. *J. Appl. Phys.* **1965**, *36* (1), 157−161.
(63) Akbar, F. I.; Aslandukova, A.; Aslandukov, A.; Yin, Y.; Trybel, F.; Khandarkhaeva, S.; Fedotenko, T.; Laniel, D.; Bykov, M.; Bykova, E.; Dubrovinskaia, N.; Dubrovinsky, L. High-Pressure Synthesis of Dysprosium Carbides. *Front. Chem.* **2023**, *11*, 1−9.
(64) Akbar, F. I.; Aslandukova, A.; Yin, Y.; Aslandukov, A.; Laniel, D.; Bykova, E.; Bykov, M.; Bright, E. L.; Wright, J.; Comboni, D.; Hanfland, M.; Dubrovinskaia, N.; Dubrovinsky, L. High-Pressure Dysprosium Carbides Containing Carbon Dimers, Trimers, Chains, and Ribbons. *Carbon* **2024**, *228*, 119374.
(65) Adachi, G.-Y.; Imanaka, N.; Fuzhong, Z.Chapter 99 Rare Earth Carbides*Handbook on the Physics and Chemistry of Rare Earth-s*Elsevier19911561−189
(66) Benson, D.; Li, Y.; Luo, W.; Ahuja, R.; Svensson, G.; Häussermann, U. Lithium and Calcium Carbides with Polymeric Carbon Structures. *Inorg. Chem.* **2013**, *52* (11), 6402−6406.
(67) Li, Y. L.; Wang, S. N.; Oganov, A. R.; Gou, H.; Smith, J. S.; Strobel, T. A. Investigation of Exotic Stable Calcium Carbides Using Theory and Experiment. *Nat. Commun.* **2015**, *6*, 6974.
(68) Dong, X.; Wang, L.; Li, K.; Zheng, H.; Wang, Y.; Meng, Y.; Shu, H.; Mao, H. K.; Feng, S.; Jin, C. Tailored Synthesis of the Narrowest Zigzag Graphene Nanoribbon Structure by Compressing the Lithium Acetylide under High Temperature. *J. Phys. Chem. C* **2018**, *122* (35), 20506−20512.
(69) Bykova, E.; Akbar, F. I.; Bykov, M.; Martynova, N.; Wenju, Z. Revealing Crystal Structure of Novel High-Pressure Tungsten Borides. *Eur. Synchrotron Radiat. Facil.* **2025**.
(70) Laniel, D.; Akbar, F. I.; Wenju, Z.; Jameson, C. Pressure Synthesis of Ultrahard Carbon Nitrides. *Eur. Synchrotron Radiat. Facil.* **2025**.
(71) Laniel, D.; Akbar, F. I.; Fedotenko, T. Single-Crystal X-Ray Diffraction Study of O2 up to 200 GPa. *Eur. Synchrotron Radiat. Facil.* **2025**.
(72) Aslandukov, A.; Laniel, D.; Akbar, F. I.; Spender, J.; Yin, Y. Synthesis and Single-Crystal X-Ray Diffraction Characterization of Novel Yttrium Nitrides under High Pressures up to 175 GPa. *Eur. Synchrotron Radiat. Facil.* **2025**.
(73) Akbar, F. I.; Aslandukov, A.; Laniel, D.; Liang, A.; Ranieri, U.; Yin, Y.; Wenju, Z. Synthesis and Single-Crystal X-Ray Diffraction Characterization of Novel Scandium Nitrides under High Pressures up to 175 GPa. *Eur. Synchrotron Radiat. Facil.* **2026**.
(74) Akbar, F. I.; Aslandukov, A.; Yin, Y. Structural Characterization of Alkali Halides with Polyhalogen Anions Using Single-Crystal X-Ray Diffraction at High Pressure. *Eur. Synchrotron Radiat. Facil.* **2026**.
(75) Akbar, F. I.; Aslandukov, A.; Aslandukova, A.; Dubrovinsky, L.; Milkin, P.; Minchenkova, A. Synthesis Single-Crystal X-Ray Diffraction and Mössbauer Characterization of Novel Iron Halides under High Pressure. *Eur. Synchrotron Radiat. Facil.* **2026**.
(76) Akbar, F. I.; Dubrovinsky, L.; Milkin, P.; Pantousas, A.; Zhou, W. Synthesis and Crystal Chemistry of Rare-Earth Carbonitrides at Pressures up to 120 GPa in Laser-Heated DACs. *Eur. Synchrotron Radiat. Facil.* **2027**.





https://doi.org/10.1021/acsomega.5c09373
*ACS Omega* 2026, 11, 4280−4289